ORIGINAL ARTICLE

Comparison of radon mapping methods for the delineation of radon priority areas – an exercise

Valeria Gruber[1]*, Sebastian Baumann[1], Oliver Alber[2], Christian Laubichler[2,3], Peter Bossew[4], Eric Petermann[4], Giancarlo Ciotoli[5], Alcides Pereira[6], Filipa Domingos[6], François Tondeur[7], Giorgia Cinelli[8], Alicia Fernandez[9], Carlos Sainz[9] and Luis Quindos-Poncela[9]

[1]Austrian Agency for Health and Food Safety (AGES), Linz, Austria; [2]Austrian Agency for Health and Food Safety (AGES), Graz ,Austria; [3]LEC GmbH, Graz, Austria; [4]German Federal Office for Radiation Protection (BfS), Berlin, Germany; [5]Italian National Research Council, CNR-IGAG, Rome, Italy; [6]University of Coimbra, CITEUC, Coimbra, Portugal; [7]ISIB-HE2B, Brussels, Belgium; [8]European Commission, Joint Research Centre (JRC), Ispra, Italy; [9]University of Cantabria, Santander, Spain

Abstract

Background: Many different methods are applied for radon mapping depending on the purpose of the map and the data that are available. In addition, the definitions of radon priority areas (RPA) in EU Member States, as requested in the new European EURATOM BSS (1), are diverse.

Objective: 1) Comparison of methods for mapping geogenic and indoor radon, 2) the possible transferability of a mapping method developed in one region to other regions and 3) the evaluation of the impact of different mapping methods on the delineation of RPAs.

Design: Different mapping methods and several RPA definitions were applied to the same data sets from six municipalities in Austria and Cantabria, Spain.

Results: Some mapping methods revealed a satisfying degree of agreement, but relevant differences were also observed. The chosen threshold for RPA classification has a major impact, depending on the level of radon concentration in the area. The resulting maps were compared regarding the spatial estimates and the delineation of RPAs.

Conclusions: Not every mapping method is suitable for every available data set. Data robustness and harmonisation are the main requirements, especially if the used data set is not designed for a specific technique. Different mapping methods often deliver similar results in RPA classification. The definition of thresholds for the classification and delineation of RPAs is a guidance factor in the mapping process and is as relevant as harmonising mapping methods depending on the radon levels in the area.

Keywords: *radon; mapping; prediction; interpolation; radon priority areas; risk; hazard*

The European Council Directive 2013/59/EURATOM (EU-BSS) (1) requires (art. 103) that member states identify areas where the radon concentration in a significant number of buildings is expected to exceed the relevant national reference levels (RL). These areas are in practice referred to as radon priority areas (RPA). Definition and delineation of RPA is relevant, because specific (mandatory) measures of the radon strategy of countries depend on it (e.g. radon measurements at workplaces, preventive measures and awareness programs). Therefore, the delineation of RPA is an important task within the transposition of EU-BSS and radon action plans in the countries, which should be implemented appropriately, accurately and reliably.

The definition of RPA in the EU-BSS allows a wide range of interpretation, and therefore, different concepts and methodologies have been proposed and already adopted in some countries (2, 3). Radon maps have existed in several countries for many years as part of national radon strategies even before the new EU-BSS became effective (4–10). The applied mapping methods and the visualisation are very different among the various countries, depending on the purpose of the map and the data available (11). These methods are based on different developments, strategies and ideas in radon protection for many years in the countries, and most of the time, the basic mapping strategies and methods applied in a country remain unchanged, even when revised or new legal requirements

were applied. Consequently, a basic bottom-up harmonisation approach (same methodology everywhere) of mapping methods or definition of RPA will not be enforceable. Therefore, comparison, evaluation and discussion for possibilities of top-down harmonisation (different methodologies are normalised to common standards) are important. Harmonised evaluation, classification and display of the radon potential are important for better comparability and compatibility between regions or countries and should serve as a basis for appropriate and consistent radon protection measures for the population. Within the European research project 'Metrology for Radon Monitoring (MetroRADON)' (12), the goal was to develop reliable techniques and methodologies to enable SI traceable radon measurements and calibrations at low radon concentrations, including also the task of harmonisation of radon data and RPA. The aim was to develop a strategy to harmonise defined RPA across borders. In this framework, studies and exercises were carried out based on literature, available data and case studies as a basis to evaluate the situation and develop strategies. Results of these studies are reported in the MetroRADON deliverable (13) and will also be discussed in journal articles, for example, the topic of causes and effects of lack of compatibility between maps and possible methods for harmonisation (14). In this article, the results of the 'radon mapping exercise' carried out within MetroRADON are presented and discussed. The idea of the exercise was to evaluate if available and established mapping methods can be applied to a data set from another area and if different mapping methods applied on the same data deliver comparable results. So, different radon mapping methods already used in countries for RPA definitions were applied to two harmonised data sets of various variables (e.g. indoor radon,

gamma dose rate, geology, soil gas radon [SGR]) to evaluate the impact of the different techniques on the delineation of RPAs, as well as their potential applications to other countries.

Material and methods

Data set description

The basis for the realisation of the mapping exercise was the availability of suitable data sets. The demands were: to have more than one data set, preferably from different countries or regions; the data set should include various variables which could be interesting for mapping (e.g. information about indoor radon, SGR, geology, geogenic parameters); and to have the permission that the data set can be shared with the participants of the exercise and the results used for the project. Based on these requirements, the selected data sets for the mapping exercise are from different radon measurement campaigns in six municipalities in Austria and in Cantabria, Spain.

The data include indoor radon concentration (IRC) measurements in dwellings, building characteristics of measured dwellings, SGR concentration, soil permeability, radionuclide concentrations (^{226}Ra, ^{228}Ra, ^{210}Pb, ^{228}Th, ^{232}Th, ^{238}U, ^{40}K) in soil samples, ambient dose rate (ADR) and maps of geology, soil type and airborne radiometry (see Table 1). All data are georeferenced and provided in shape files or TIFF raster files.

The Austrian data set covers six municipalities and is separated into two distinct areas located in the North and in the South of Austria (AUT North and AUT South, respectively, Fig. 1, bottom). Each area consists of three adjacent municipalities with an overall area of about 220 km² (40 km² in AUT North, 180 km² in AUT South).

Table 1. Overview of existing variables in the Cantabrian and the Austrian data set

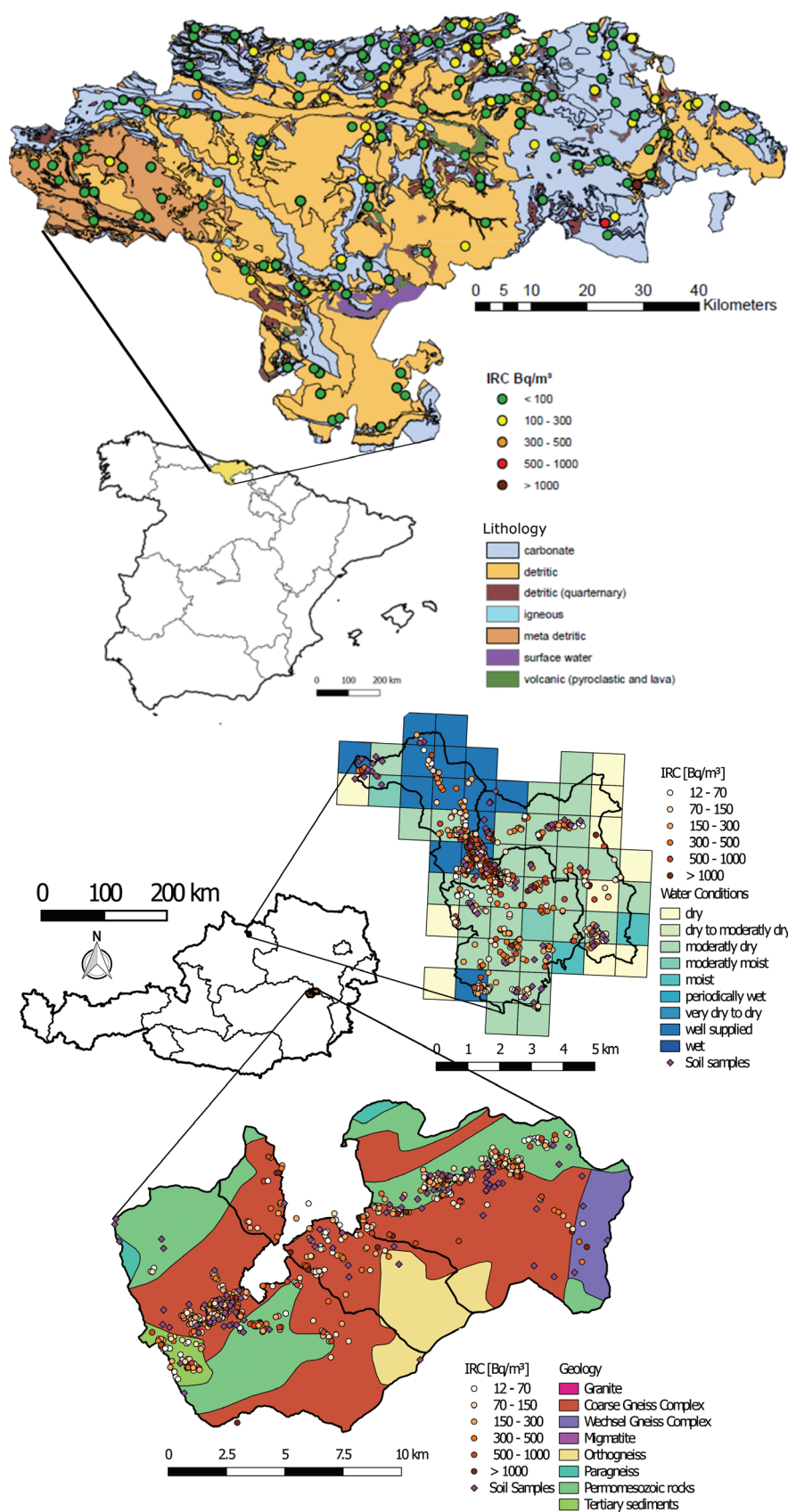| Variable	Cantabria	Austria (AUT North and AUT South)
Indoor radon concentration (IRC)	*Measured*; 482 dwellings, approximate location, low sample density (0.09/km²) (21)	*Measured*, 1.638 dwellings, exact location, high sample density (7.44/km²)
Soil gas radon (SGR)	*Measured*; 260 locations, sample density similar (0.05/km²)	*Measured*; 148 locations, sample density similar (0.67/km²)
Soil permeability	Estimated from lithological units (25)	*Measured*; 148 locations
Activity concentration of radionuclides in soil	European K, Th, U in soil maps (26) 10 × 10 km grid arithmetic mean (AM)/geometric mean (GM) (based on (27, 28)	*Measured*; 112 locations, ^{40}K, ^{210}Pb, ^{226}Ra, ^{228}Ra, ^{228}Th, ^{238}U
Ambient dose rate (ADR)	*Measured*; MARNA map (24, 29), sample density similar	*Measured*; 148 locations, sample density similar
eU	-	*Measured*; only in AUT North; by airborne radiometry (30)
Faults	Map 1:1.000.000 (31), similar	Map 1:500.000 (32), similar
Geology	Map 1:200.000 (22), similar	Map 1:500.000 (32), similar
Karst	Binary, derived from lithological units (33)	-
Building characteristics	-	Questionnaire; at location of IRC
Soil map	-	Soil map 1 × 1 km grid (34), various variables (e.g. soil type, soil water content, permeability, soil depth)

Fig. 1. Top: The map of Cantabria with selected variables and the position of Cantabria in Spain. Bottom: The Austrian data set with selected variables and a map of Austria showing the position of the areas AUT North and AUT South.

Most of the data were collected during detailed measurement campaigns carried out between 2010 and 2012. The survey data are supplemented with data obtained from literature (see Table 1). The area AUT North is located in the Bohemian Massif which is characterised by high geogenic radon potential (GRP) due to the predominant presence of granites and gneiss outcrops. It shows homogeneous geological features with a granitic pluton and interlaying migmatites (metamorphic rocks with granitic parent rock). The geology of AUT South is comparatively heterogeneous and is characterised by a variety of felsic igneous and metamorphic rocks with high radon potential, but also sedimentary units with low radon potential. References to the geological maps are given in Table 1. More details about the radon survey and data are discussed in Refs. (15–19) and more information about radon and geology in Austria are given in Ref. (10, 20).

The Spanish data set covers the region of Cantabria (Fig. 1, top) having a total area of about 5,300 km². The data set consists of different measurements of IRC, SGR, ADR and data compiled from literature (see Table 1). The geology of Cantabria is mainly characterised by detritic sediments and carbonate rocks, which usually show low to intermediate radon potential; however, the high permeability of the fractured carbonates can result in locally higher GRP. The metasediments located in the western part of the region and local volcanoclastic formations usually show a low GRP. In general, compared to the Austrian regions, Cantabria has lower GRP. References to the geological maps are given in Table 1. More details about radon mapping in Spain are discussed in (21–24).

Figure 1 shows the studied areas in Austria and Spain. The figure also includes classed post maps of the the IRC measurements and examples of other available data layers (e.g. geology, water conditions and lithology).

The data sets differ in basic characteristics such as size, sample density, quality and resolution. The characterisation of RPA for the two data sets may require adequate data preparation according to the different mapping methods. Table 1 reports an overview and a comparison of the Austrian and the Cantabrian data sets regarding data density, similarity, source (e.g. measured or derived from literature) and number of measurements (where applicable).

Detailed analyses were carried out for all variables of all data sets (AUT North, AUT South, Cantabria). Descriptive statistical analysis was performed by box-plot graphs and by other statistical methods (Kruskal–Wallis test, Spearman's rank correlation, variograms). Details can be found in the final report of the exercise (35). Table 2 shows a qualitative summary of the statistical and spatial correlations of the analysed variables. The analysis of the datasets indicates that the different regions do not show the same results regarding the correlation between

quantities, differences of a quantity within groups (e.g. bedrock type, soil grain size, water content in the soil, permeability, building characteristics) and strength of spatial correlations.

Methods
Different mapping methods are discussed within the exercise. The idea was to include as many mapping methods as possible in the exercise, which were already used for radon mapping in countries or were suggested by experts. Therefore, experts from different countries were invited to participate in the exercise and apply their respective mapping method to the provided exercise data sets. Not all invited experts had the time or resources to perform the exercise (as we could not provide funding for the external participants for this work within the project). The mapping methods and results of those who agreed to participate in the exercise were included in this article. In addition, basic statistics of indoor radon data was performed, as basic statistic methods are also used for radon mapping in several countries.

In the following, these methods are briefly described, and examples of comparisons are examined in the Results section. More details about the methods and results can be found in the final report of the exercise within the MetroRADON project (35) and the reported specific literature.

Basic Statistics of Indoor Radon Data
The definition of RPA by using IRC data commonly follows one of two basic concepts: 1) the mean IRC (e.g. AM, GM) of the area is compared to a threshold (e.g. 300 Bq/m³) and 2) the percentage of measurements exceeding a threshold (RL) in an area is compared to a percentage threshold (e.g. 10%). Common approaches to define RPA use IRC thresholds (RLs) ranging from 100 to 300 Bq/m³ and percentage thresholds ranging from 1% to 30%. Descriptive statistical analysis was performed for the exercise data in the light of these two basic RPA concepts, as a common mapping method. Results are shown in Table 3 and Fig. 2.

Generalised Additive Mixed Model (GAMM)
GAMM (36) is used to estimate the IRC (as a dependent variable) by using the correlation with some explanatory variables. The method is based on Ref. (37). For Austria, the additive mixed model:

$$\log(IRC_{ij}) = \beta_0 + \beta_1 z_{1,ij} + ... + \beta_m z_{m,ij} + s(x_j, y_j) + u_j + \epsilon_{ij}$$

$$j = 1,...,n_{house} \quad i = 1,...,n_{j,room} \quad u_j \sim N(0, \sigma_{house}^2) \quad \epsilon_{ij} \sim N(0, \sigma_{\epsilon}^2)$$

is fitted to the data set, whereby the living unit u_j is taken as a random effect, thus introducing a positive correlation

Table 2. Significant differences within groups, significant correlations (general positive, negative correlations are indicated by [-]) and strength of spatial correlation in the different regions

| Quantity	Significant difference of quantity within groups of	Significant correlation with	Spatial auto-correlation
AUT North			
Ambient dose rate (ADR)	Bedrock types, soil source type	K-40, Th-228, Ra-228, TGDR	Weak
eU	Bedrock type, soil source type	x	Strong
Soil gas radon (SGR)	Soil type, soil grain size, soil water content	U-238	Weak
Pb-210	Bedrock type	U-238, Ra-226	No
Ra-226	x	U-238, Ra-226	No
U-238	x	SGR, Ra-226, Pb-210	No
Terrestrial Gamma Dose Rate (TGDR)	x	ADR, K-40, Ra-228, Th-228	No
Indoor radon concentration (IRC)	Permeability, bedrock type, soil water content, some building characteristics	x	Weak
AUT South			
ADR	Bedrock type	Soil gas, Ra-226, TGDR	Weak
soil gas	x	ADR, K-40, Pb-210, Ra-226, U-238, TGDR	No
Pb-210	x	SGR, K-40, Ra-226, Pb-210, Ra-228, U-238, TGDR	No
Ra-226	x	SGR, ADR, K-40, Ra-226, K-40, Pb-210, Ra-228, Th-228, U-238, TGDR	No
Ra-228	Soil source type, soil grain size	K-40, Ra-226, Th-228, U-238, TGDR	No
Th-228	Soil source type, soil grain size	Ra-226, Ra-228, U-238, TGDR	No
U-238	x	SGR, K-40, Pb-210, Ra-226, Ra-228, Th-228, TGDR	No
TGDR	x	soil gas, ADR, K-40, Ra-226, K-40, Pb-210, Ra-228, Th-228, U-238, TGDR	Weak
Indoor radon concentration (IRC)	Some building characteristics	x	No
Cantabria			
ADR	Lithology, source, permeability	SGR (-), Th, K	Strong
Soil gas	Lithology, source, permeability	IRC, ADR (-), U (-)	No
IRC	Lithology, karst	SGR, U (-)	No

'x' indicates no observation.
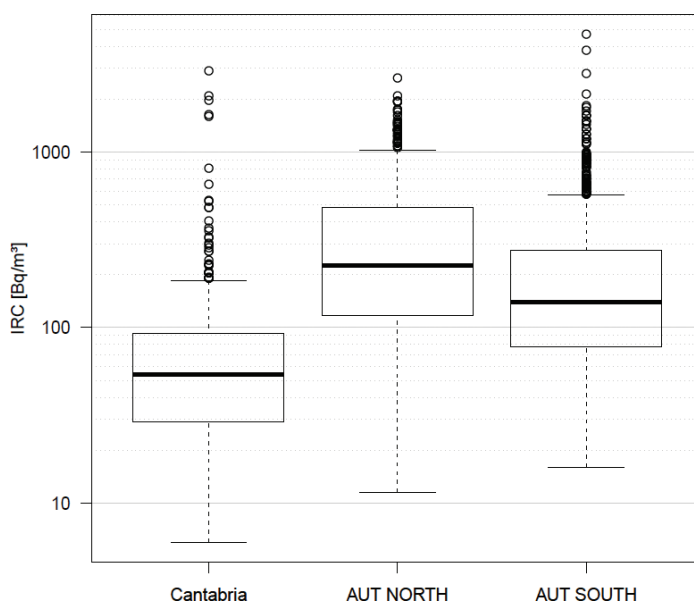
Fig. 2. Boxplot showing indoor radon concentration distributions in log scale for the different regions of the exercise data.

of measurements within the same living unit, because u_j is common to all measurements within unit (j). A slightly different additive model without random effects is used for the Cantabrian data set, because measurements from a relatively large area are assigned to a particular location. Influencing factors, such as geology, in such an area could be inherently different, which would contradict the positive correlation induced by the random effect. In both cases, the smooth functions s(.) pertain to the class of thin plate regression splines. The z_{ij} terms represent explanatory variables and the pair (x_j, y_j) represents the coordinates of a living unit or location j. The final model should only contain variables that show a significant influence on log(IRC). To identify these variables, a stepwise forward selection using a 5-fold random cross validation was applied. Variables with the highest explanatory power were chosen for the final model. Non-relevant variables result in non-significant improvements in cross validation error.

For Cantabria, the following explanatory variables based on the fivefold random cross validation were used for the final model: soil-type, ADR, K_2O and Th content in soil. For the Austrian data sets, the following building characteristics were used: room earthbound (yes/no), floor, type of walls, type of basement (yes/no/partly), solitary building (yes/no) and type of bedrock. Additionally, the type of foundation and the U content were selected for the AUT North data set, while the fraction of measurement time in winter, the number of dwelling units, tightness of windows and water saturation of the soil were selected for the AUT South data set. The final models are fitted using these variables to predict log(IRC) according to specified grids (10 × 10 km for Cantabria and 2 × 2 km for Austria). Some results can be found in Table 3.

Ordinary Kriging (OK) and Indicator Kriging (IK)

The kriging method (38–40) was performed for the prediction of IRC in both Austria and Cantabria. For Austria,

an analysis of variance (ANOVA) was performed for the following target variables: IRC (only ground floor measurements were considered), SGR, soil permeability and the GRP after (41) (as function of SGR and soil permeability). ANOVA revealed significant ($P < 0.05$) differences for the target variables dependent on pedology and geology. Considering the high density of IRC measurements in populated areas, a pure geostatistical approach using OK and IK without any additional predictor seemed to be sufficient to estimate the radon risk for populated areas. First, the spatial autocorrelation of IRC was tested by calculating variograms. Based on these variogram models and the empirical data, IRC was kriged for a raster cell size of 200 m. Due to the low range of spatial autocorrelation, the estimates at large distances from the nearest observation (> 1 km) are equivalent to the mean of the whole area. The radon risk mapping was conducted using IK. For this purpose, IRC was transformed into a binary code with 0 for all observations that are smaller than 300 Bq/m³ and 1 for all observations that are greater or equal to 300 Bq/m³. Another variogram model was fitted to the binary coded data.

As the IRC data from Cantabria have no exact coordinates and no information was available about the floor of the building in which the measurement was performed, a different method was used. To make the data ready for kriging, all measurements from one municipality were merged into one value by calculating the arithmetic mean (AM). Thus, each unique location is assigned to one value for IRC. Spatial autocorrelation of IRC was tested but not detected, that is, the empirical data could not be fitted in a meaningful way to the variogram model. Hence, kriging of IRC was not a feasible option for the delineation of radon risk areas in Cantabria. Instead of a geostatistical analysis of IRC, the GRP was calculated as a function of SGR and soil permeability. Kriging, based on an exponential variogram model, was conducted for SGR.

Table 3. Results for different methods and regions for indoor radon concentration in Austria and Spain

	AM (Bq/m³) DS	GM (Bq/m³) DS	Med (Bq/m³) DS	% > 300 DS	Med (Bq/m³) BRRMS	% > 300 BRRMS	GM (Bq/m³) GAMM	AM (Bq/m³) OK	% > 300 IK
Cantabria	97	54	54	3	-	-	54	-	-
AUT North Mun.1	289	196	197	31	231	40	243	352	36
AUT North Mun. 2	313	207	213	36	240	41	201	360	39
AUT North Mun. 3	429	273	266	45	230	39	208	367	39
AUT South Mun. 4	289	165	168	28	209	38	153	305	26
AUT South Mun. 5	251	157	144	22	183	32	241	300	26
AUT South Mun. 6	234	146	130	21	173	31	310	304	26

AM, arithmetic mean; GM, geometric mean; Med, median; DS, descriptive statistics.

Data on soil permeability was assigned to five permeability classes, depending on the lithological type. Consequently, it was not possible to use the Neznal GRP (41). According to the Cantabrian data set, the GRP was defined as:

$$GRP = Soil\ Rn * Permeability^2.$$

Examples of the results by Kriging methods are shown in Fig. 4 (left hand side) and Fig. 7 (right hand side).

Empirical Bayesian Kriging Regression (EBKR)

EBKR is a geostatistical interpolation method that combines kriging interpolation and ordinary least square regression providing an accurate prediction of moderately non-stationary data at a local scale. It uses a dependent variable measured at point locations and known potentially correlated explanatory variables, as raster grids (42, 43). EBKR estimates multiple semivariogram models instead of a single variogram by repeated simulations, thus accounting for the uncertainty introduced in the calculation of variogram parameters and providing a better accuracy than other kriging techniques. In common kriging methods, the prediction at unknown locations considers the nearby known data. This may result in the underestimation of the prediction standard errors caused by the uncertainty of semivariogram parameters. In contrast, EBK uses an intrinsic random function as the kriging model, differently than the other kriging methods, and does not assume a tendency toward the overall mean; this results in the same probability for large deviations to get larger or smaller. Furthermore, EBKR also considers the presence of a multicollinearity among the explanatory variables by using the principal components in the regression model. Each principal component captures a certain proportion of the total variability (set to 75%) of the explanatory variables. Cross-validation method was used to estimate the performance of the model.

In this work, the estimation by EBKR uses radon concentration in soil gas as response variable and raster layers of permeability, ADR, K-40, U-238, Th-232, fault density, presence of karst areas as predictors with a resolution of 500×500 m. Figure 4 (right hand side) shows the result of EBKR for GRP mapping of Cantabria.

Belgian Radon Risk Mapping Software (BRRMS)

Cinelli et al. (44) developed the method and the corresponding software is described in Ref. (45). The principle is to map the variations of the radon risk within geological units with the moving average method, while geological units with significantly different levels of risk are considered separately. When contiguous geological units have similar mean IRC levels, they are treated as a single unit. Within a given unit, the moving average of the nearest 20 data points is calculated (more precisely, the log mean, or the log median) for any chosen coordinate set, for example, the nodes of a square grid. The percentage of data locally exceeding a chosen threshold is also predicted, assuming lognormal distribution. The threshold used in the exercise is the European reference level of 300 Bq/m³, and the lognormal distribution is only fitted to data above the median (46). The method does not include a classification of the nodes. A classification in five risk classes is used in the Belgian method for municipalities (47), but was not included in the software.

Only the Austrian data set was used for this method, and only the highest concentration, measured on the ground floor, was kept for each living unit. The Austrian data sets are from two distinct rather small radon-affected areas. Each area includes different geological formations. However, the radon statistics give rather similar values for the geometrical mean (GM) IRC in the different geological units of each area, and therefore, they were considered as a single mapping unit. In Fig. 7 (left hand side), one example of the results is shown.

Results and discussion

The data sets for the exercise are complex, and correlations between variables were less significant than expected (Table 2). The Austrian data sets represent only small areas (6 municipalities), which seems to be too small and geologically homogenous with respect to radon risk for geogenic correlations and modelling. The Cantabrian data set represents a larger area, but the data came from different surveys and literature (see Table 1). In addition, the Cantabrian data set has low sampling density and no exact coordinates for IRC, which makes the use of IRC for modelling challenging.

The fact that the data are inhomogeneous and not perfect in several aspects makes the exercise realistic, since, in practice, most of the time the available data for mapping are neither as perfect nor as complete as would be desirable. Consequently, the exercise shows how mapping methods can perform with incomplete or heterogeneous data sets, and how the classification of RPA can be done with them.

The data sets required adequate data manipulations to apply the different mapping methods, and not all data were used for each mapping method. Further, certain data characteristics (e.g. different input variables, not all variables which are needed for a method exist in all data sets) inhibit the application of each mapping method for every dataset. Table 4 gives an overview of the applied mapping methods and the data that were used for the respective method. In general, mapping methods are mostly specified to use either IRC or geogenic variables as input variables. The BRRMS combines IRC and geogenic variables by considering geological units. The methods using IRC

Table 4. Overview of different methods and variables used in the respective method

Method	Indoor radon concentration (IRC)	Building characteristics	Soil gas radon (SGR)	Radionuclide contents	Geogenic factors	Interpolation
IRC mean over threshold	Yes	Possible subset data	No	No	No	No
Probability of IRC over threshold	Yes	Possible subset data	No	No	No	No
GAMM	Yes	Yes	Yes	Yes	Yes	Yes
EBKRP	No	No	Yes	Yes	Yes	Yes
Kriging IRC (AT)	Yes	Subset data	No	No	No	Yes
Kriging GRP (ES)	No	No	Yes	Yes	Yes	Yes
Belgian radon risk mapping software (BRRMS)	Yes	Subset data	No	No	Yes	Yes

with building characteristics could only be applied for the Austrian data sets, as no information about building characteristics is included in the Cantabrian data set. Only the GAMM method used all available variables for the Austria and the Cantabrian data sets and selected the relevant explanatory variables in a stepwise forward method. Apart from the basic statistic methods, all applied methods used interpolations to map the radon concentration, radon potential or the radon risk.

A summary of the results for Cantabria and the six municipalities in Austria for IRC derived from the different methods is shown in Table 3. The table gives an arithmetic/geometric mean/median value for the IRC or the percentage of measurements above 300 Bq/m³ in Cantabria and each of the six Austrian municipalities (Mun.). The methods which delivered results for grid cells were aggregated for the region of Cantabria and the municipalities in Austria. For this purpose, all grid cells were used, and the target variable of the corresponding method (median, geometric mean, arithmetic mean) was used as aggregate. This simple approach was chosen only to give an overview of the results derived from different methods based on administrative areas (province, municipalities), which RPA delineation is mostly based on. The results show that the predicted radon concentration is clearly lower for all methods in Cantabria than in Austria (see also Fig. 2) and also lower in the three municipalities in AUT South compared to AUT North. The GM of Cantabria data from basic statistics and the GAMM correspond very well, also for AUT Mun. 2 and 4. For the other municipalities, it deviates quite strongly, especially for Mun. 5 and 6. The BRRMS median (Med) concentration per municipality compared to basic statistics median deviates about 10–30%, and the deviation is stronger for the values of percentages above 300 Bq/m³. The OK IRC and BRRMS IRC predictions per municipality deliver higher values than the basic statistics, except for Mun. 3.

In the following, we will describe the consistency/comparability of different methods through a few examples.
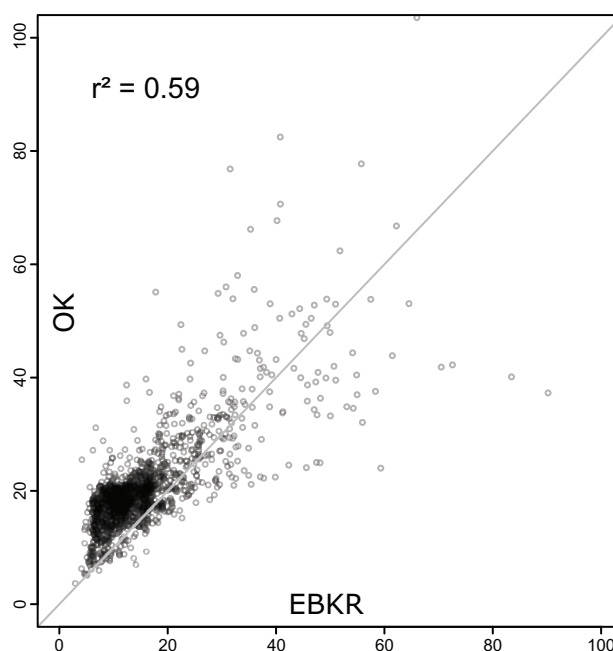
Fig. 3. Correlation between two different mapping methods for the GRP for Cantabria data set – OK vs. EBKR.

Correlation analysis was performed only for methods, which provided the same variable as result (IRC, GRP) and the results were aggregated to the same grid.

Figure 3 compares the GRP predictions for Cantabria obtained by applying EBKR and OK. The data were aggregated into a 5 × 5 km grid and the coefficient of determination (R^2) is 0.59. The correlation between the two methods for the area is good (acceptable). The GRP predictions of the two methods are displayed in the map in Fig. 4. The two maps show a corresponding pattern, with only some higher GRP in the North of Cantabria. OK predictions are generally higher for the central and southern part of Cantabria (Fig. 5). Possible reasons for this observation are seen as 1) utilisation of co-variable data by EBKR but not by OK and 2) predictions by OK beyond the range of spatial auto-correlation. In more
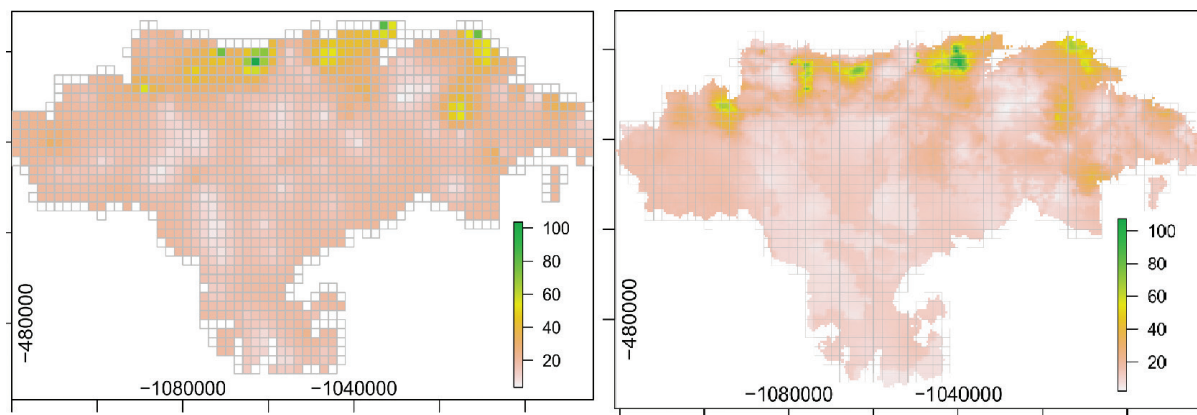
Fig. 4. Mapping the GRP prediction in 5 × 5 km grid for Cantabria with OK (left hand side) and EBKR (right hand side). Predictions were aggregated into 5 × 5 km grids.
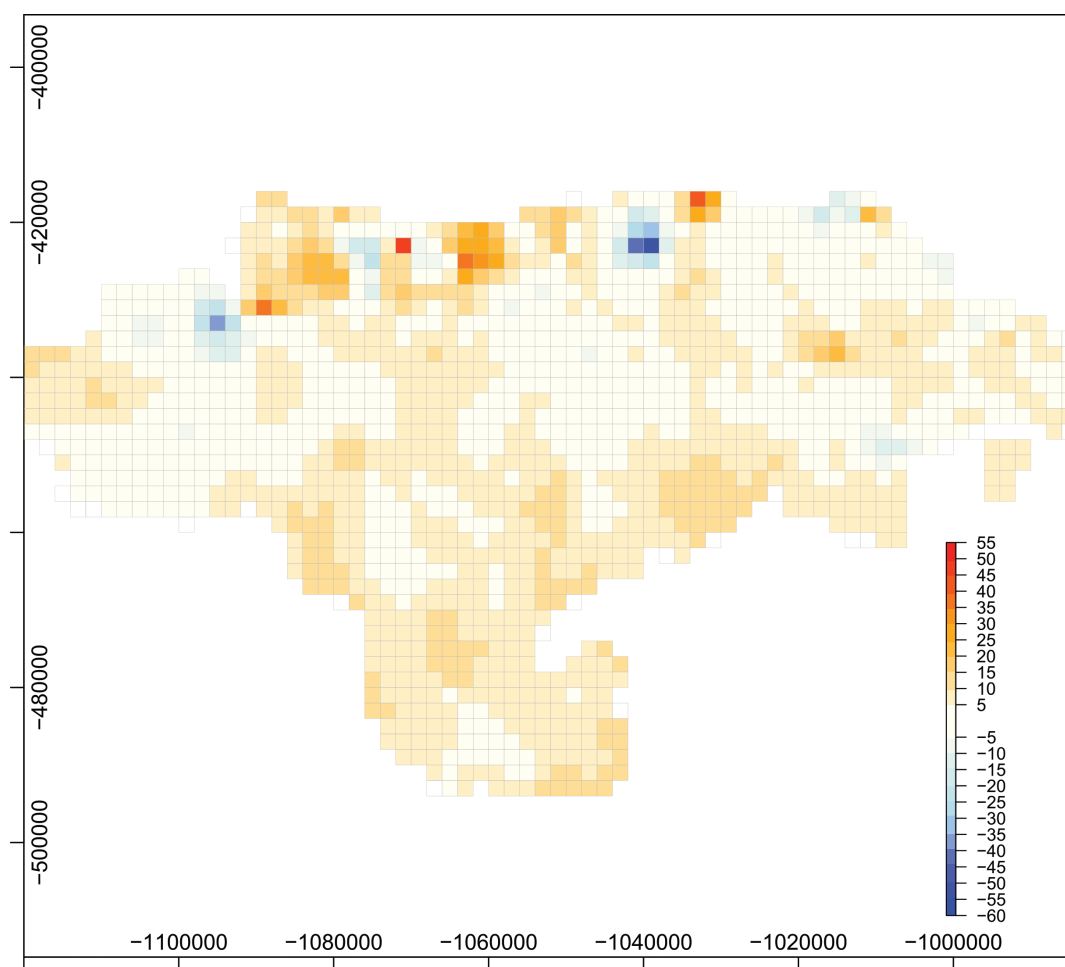

Fig. 5. Absolute difference of the GRP prediction results in 5 × 5 km grid for Cantabria of OK (Fig. 4, left hand side) and EBKR (Fig. 4, right hand side).

detail, for 1) OK uses only nearby observations for predictions whereas EBKR considers many environmental co-variables (such as geology). If, for instance, a geological unit with a small spatial extent and medium/too high

risk exists within an area with general low risk, for OK a single medium/high Rn measurement would affect the whole area within the range of spatial auto-correlation by increasing the estimate irrespective of the environmental

setting. In contrast, for EBKR higher predictions would be more restricted to the respective geological unit where the medium/high Rn concentration was observed. For 2) low sampling density in certain areas could result in some cells being located beyond the range of spatial auto-correlation. This would be especially problematic for OK,
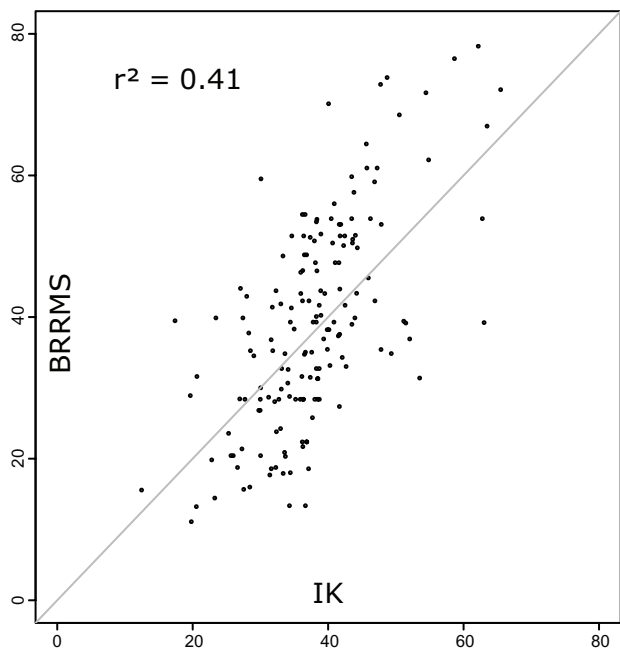
because for these cells, the OK estimate tends towards the mean of the observational data. The mean of the observational data might in turn be influenced by more measurements from high Rn concentration areas (in case of Cantabria more measurements were conducted in the north where Rn concentration is higher).

A detailed evaluation of performance of the individual maps in terms of its actual accuracy would have required independent test data that are currently not available or exhaustive simulation (e.g. via repeated cross-validation), which was beyond the scope of this study. However, performance assessment for different mapping methods applied for radon risk evaluation is certainly an important task that deserves a more detailed analysis in the future.

Figure 6 compares the BRRMS method with the IK method for the predicted percentage of measurements above 300 Bq/m³ for the area AUT North. As basis for comparison, the coarser 500×500 m grid of the BRRMS was used and compared with the cell of the 200×200 m kriging raster closest to the midpoint of the BRRMS grid cell. The coefficient of determination (R^2) is 0.41, which is still a satisfying correlation. In Figure 7, the results of the two methods are displayed as maps. The two maps are similar, showing the highest radon potential in the centre. In general, the predicted IRC by the BRRMS method is higher than the one by IK.

Finally, we evaluated how the different results provided by different mapping methods would have an impact on the classification or delineation of RPAs. As discussed above, different definitions of RPA concepts were chosen
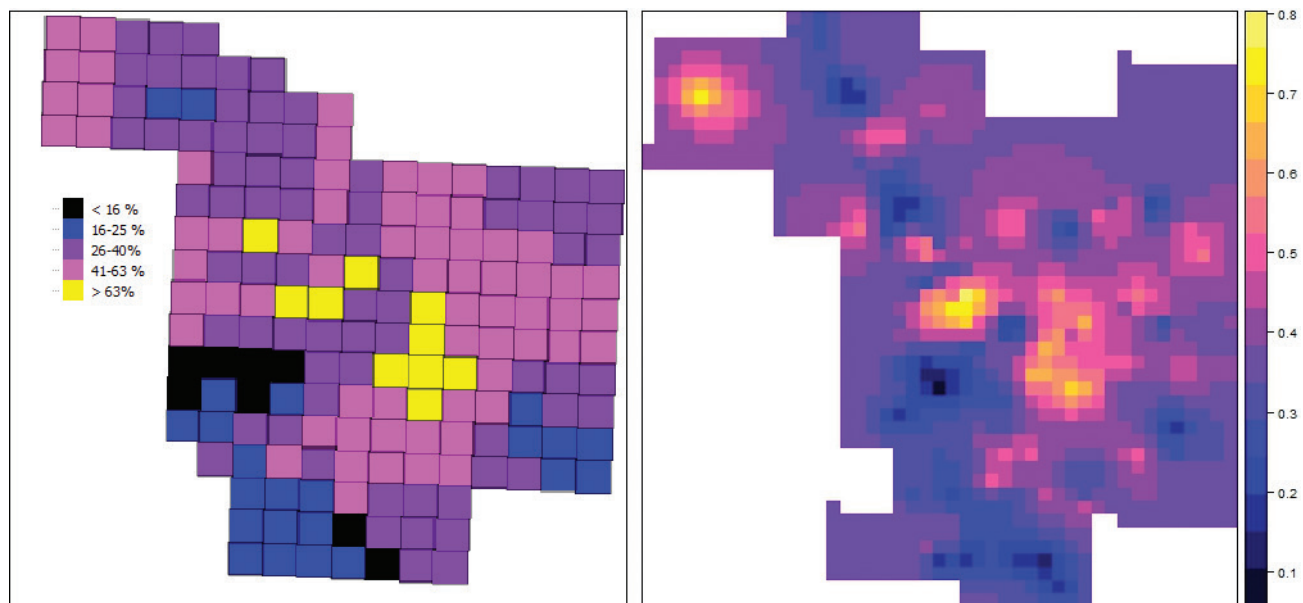

Fig. 6. Belgian Radon Risk Mapping Software (BRRMS) vs. Indicator Kriging (IK).

Fig. 7. Mapping the prediction of % above 300 Bq/m³ for the AUT North data set with Belgian Radon Risk Mapping Software (BRRMS, left hand side) and Indicator Kriging (IK, right hand side).

in the individual countries. We adapted two RPA classification definitions to the results for IRC of the different methods shown in Table 2. If the threshold of AM/Med/GM is set to 300 Bq/m³, results highlight that: 1) all six Austrian municipalities would be classified as RPA with the OK method; 2) mun. 2 and 3 would be classified as RPA with the basic statistics method (AM); 3) mun. 6 would be classified as RPA with the GAMM method. If the threshold of above AM/Med/GM is set to 100 Bq/m³, results show that all six Austrian municipalities with all applied methods would be classified as RPAs. Cantabria

would not be considered as RPA for all these methods and classification thresholds. These results highlight that the threshold chosen for the classification of RPA has a major impact on RPA delineation, depending on the level of radon concentration in the area. For Cantabria, which has a very low IRC, the different results obtained by applying different methods do not impact the RPA classification. In contrast, the Austrian municipalities show radon concentrations in the range about 150–400 Bq/m³, depending on municipality and mapping method. Differences in the radon concentration (even when small)
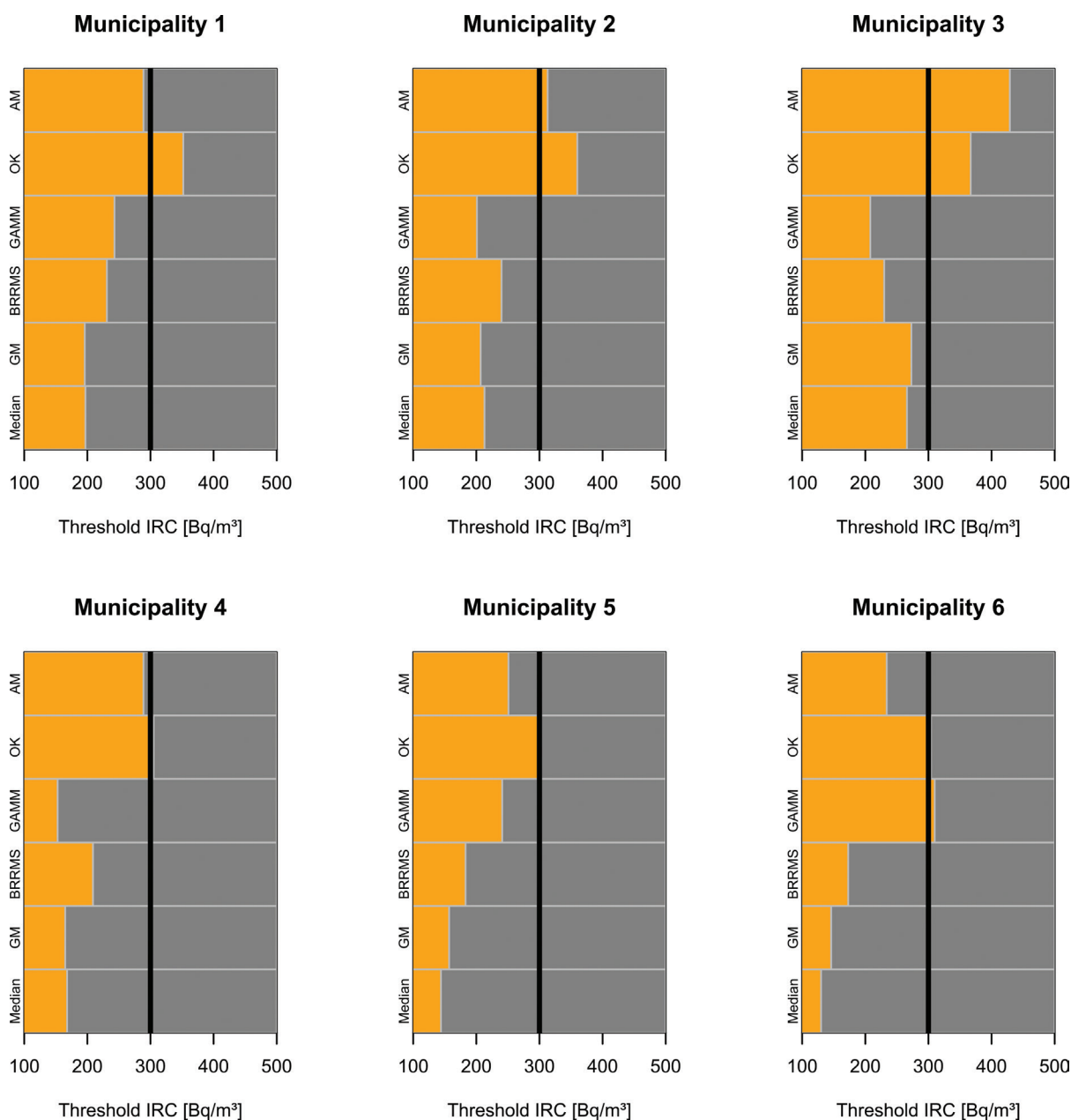

Fig. 8. Classification of RPA for the 6 municipalities in Austria with different methods and for different thresholds (grey: no RPA, orange: RPA – further explanation in the text).

for the different methods for the same municipality impact the RPA classification, when the threshold is chosen in the range of the variability of the results (e.g. 300 Bq/m³, as shown in the example). If the threshold is set to 100 Bq/m³, all municipalities are classified the same, as this threshold does not lie within the range of the measurement/prediction results, and therefore, the variability of the results among the different methods does not impact the classification of RPAs.

If the threshold of percentage of measurements/predictions is set to 30% (over 300 Bq/m³), all municipalities in AUT North would be classified as RPAs with all three applied methods, as well as all six municipalities for the BRRMS method. Applying the commonly used definition of RPA in Europe (10% of dwellings above 300 Bq/m³), all six municipalities in Austria would clearly be considered as RPAs, independent of the mapping method. As discussed above, the variability of the results of the different methods only impacts the classification of RPA when the set threshold lies within the range of the predicted/measured results.

Figure 8 displays the results for the three municipalities of the AUT North and Austria South areas for the different methods. The results (AM/GM/Med) per municipality for the respective methods are plotted, and the colouring shows for which threshold the municipality would be considered to be RPA (orange) and non-RPA (grey).

Conclusions

The evaluation of IRC and GRP in Europe and their harmonisation between countries and across borders constituted one of the main objectives of the MetroRADON project. This exercise-work, conducted within a specific task of the project, was aimed at the definitions of RPAs by using different mapping techniques. Results highlight that the application of a mapping method using data sets, not designed for the specific requirements of the used mapping method, is challenging. Usually, data sets always have specific characteristics and are rarely comparable, even for the same variable. Therefore, harmonisation is a challenge. However, some of the mapping methods used in this exercise show quite good correlations for the predicted cells, indicating that the used methods should in principle be interchangeable for harmonisation purposes. In general, the selection of a mapping method for a certain area will strongly depend on the available data sets and their statistical properties. Therefore, not all mapping methods are usable for all data sets or areas, depending especially on data quality, sampling density or natural heterogeneity of the mapping area. For harmonisation purposes of mapping at a European scale, a method using less parameters might be preferable, as it would be easier to apply to different data sets.

If a survey for delineation of RPA is started from scratch in a country, the mapping and display/classification methods (e.g. % above RL in administrative area) should be decided at the beginning, so that the survey design (e.g. sampling density and analysed parameters) can be optimised to these requirements.

Usually, the final goal of radon mapping is the delineation of RPAs, as this is requested in the EU-BSS. It was shown in this exercise that independent of the applied method for large intervals of classification thresholds, the same RPA classification is predicted. Different methods often deliver same results in RPA classification, according to the definition of RPAs. Problems emerge if the classification thresholds are close to mean IRC levels. In this case, small differences in estimated IRC between mapping methods can impact the RPA identification of the study area. The definition of the threshold values is an essential factor in the process of delineation of RPA. The definition of RPA is in general the most important factor that contributes to disharmony between RPA maps, and its harmonisation is as relevant as harmonising mapping methods.

Conflict of interest and funding

References

1. Council Directive 2013/59/Euratom of 5 December 2013 laying down basic safety standards for protection against the dangers arising from exposure to ionising radiation, and repealing Directives 89/618/Euratom, 90/641/Euratom, 96/29/Euratom, 97/43/Euratom and 2003/122/Euratom. Official J Eur Union L. 2014; 13(57): 1–73.

2. Bossew P. Radon priority areas – definition, estimation and uncertainty. Nucl Tech Radiat Protect 2018; 33(3): 286–92. doi: 10.2298/NTRP180515011B

3. Bochicchio F, Venoso G, Antignani S, Carpentieri C. Radon reference levels and priority areas considering optimisation and avertable lung cancers. Radiat Protect Dosim 2017; 177(1–2): 87–90. doi: 10.1093/rpd/ncx130

4. World Health Organisation (WHO). WHO handbook on indoor radon: a public health perspective. World Health Organization; 2019. Available from: https://apps.who.int/iris/handle/10665/44149 [cited 21 October 2020]

5. International Atomic Energy Agency (IAEA). Design and conduct of indoor radon surveys, safety reports series No. 98. Vienna; 2019. Available from: https://www-pub.iaea.org/MTCD/Publications/PDF/PUB1848_web.pdf [cited 21 October 2020]

6. Pantelić G, Čeliković I, Živanović M, Vukanac I, Nikolić JK, Cinelli G, et al. Qualitative overview of indoor radon surveys in

Europe. J Environ Radioact 2019; 204: 163–174. doi: 10.1016/j.jenvrad.2019.04.010

7. Pantelić G, Čeliković I, Živanović M, Vukanac I, Nikolić JK, Cinelli G, et al. Literature review of Indoor radon surveys in Europe. Luxembourg: Publications Office of the European Union; 2018. Available from: https://publications.jrc.ec.europa.eu/repository/bitstream/JRC114370/jrc114370_final_metroradon_jrc114370.pdf

8. Bossew P. Mapping the geogenic radon potential and estimation of radon prone areas in Germany. Radiat Emerg Med 2015; 4(2): 13–20. Available from: http://crss.hirosaki-u.ac.jp/wp-content/files_mf/1465449240rem_vol42_03_peter_bossew2.pdf

9. Elío J, Crowley Q, Scanlon R, Hodgson J, Long S. Logistic regression model for detecting radon prone areas in Ireland. Sci Total Environ 2018; 599–600: 1317–29. doi: 10.1016/j.scitotenv.2017.05.071

10. Friedmann H. Final results of the Austrian Radon Project. Health Phys 2005; 89(4): 339–48. doi: 10.1097/01.hp.0000167228.18113.27

11. Dubois G. An overview of radon surveys in Europe, Publications Office of the European Union. Editor: European Commission; 2005.

12. MetroRADON – Metrology for radon monitoring, project website. Available from: http://metroradon.eu [cited 21 October 2020].

13. Baumann S, Bossew P, Celikovic I, Cinelli G, Ciotoli G, Domingos F, et al. MetroRADON Deliverable 5 – Report and guideline on the definition, estimation and uncertainty of radon priority areas (RPA). 2020. Available from: http://metroradon.eu/wp-content/ uploads/2017/06/16ENV10-MetroRADON-D5-with-Annexes_ Accepted.pdf [cited: 21 October 2020]

14. Bossew P, Čeliković I, Cinelli G, Ciotoli G, Domingos F, Gruber V, et al. *On harmonization of Radon maps* (Draft submitted to JERA, January, 21 2021)

15. Ringer W, Baumgartner A, Baumgartner A, Bernreiter M, Edtstadler T, Friedmann H, et al. Radonvollerhebung in den Gemeinden Reichenau, Haibach und Ottenschlag i.M. – Expertenbericht, Technical Report. Vienna: Bundesministeriums für Land-und Forstwirtschaft, Umwelt und Wasserwirtschaft; 2011.

16. Kabrt F, Seidel C, Baumgartner A, Friedmann H, Rechberger F, Schuff M, et al. Radon soil gas measurements in a geological versatile region as basis to improve the prediction of areas with a high radon potential. Radiat Prot Dosimetry 2014; 160(1–3): 217–21. doi: 10.1093/rpd/ncu086

17. Kabrt F, Baumgartner A, Maringer FJ. Study of parameters relevant for a better prediction of the radon potential. Appl Radiat Isot 2016; 109: 444–8. doi: 10.1016/j.apradiso.2015.11.096

18. Friedmann H, Baumgartner A, Bernreiter M, Gräser J, Gruber V, Kabrt F, et al. Indoor radon, geogenic radon surrogates and geology – Investigations on their correlation. J Environ Radioact 2017; 166(Part 2): 382–9. doi: 10.1016/j.jenvrad.2016.04.028

19. Kabrt F, Baumgartner A, Stietka M, Friedmann H, Gruber V, Ringer W, et al. A comparison of radon indoor measurements with interpolated radon soil gas values using the inverse weighting method on measured results. *Radiat Protect Dosim* 2017; 177(Issue 1–2): 213–19. doi: 10.1093/rpd/ncx141

20. Dubois G, Bossew P, Friedmann H. A geostatistical autopsy of the Austrian indoor radon survey (1992–2002). Sci Total Environ 2007; 377: 368–95. doi: 10.1016/j.scitotenv.2007.02.012

21. Sainz-Fernandez C, Fernandez-Villar A, Fuente-Merino I, Gutierrez-Villanueva JL, Martin-Matarranz JL, Garcia-Talavera M, et al. The Spanish indoor radon mapping strategy.

22. Radiat Prot Dosim 2014; 162(1–2): 58–62. doi: 10.1093/rpd/ncu218

22. Spanish Nuclear Safety Council (CSN). Natural radiation maps. Viewer: Spanish radon potential map; 2017. Available from: https://www.csn.es/mapa-del-potencial-de-radon-en-espana [cited 21 October 2020]

23. Sainz Fernández C, Quindós Poncela LS, Fernández Villar A, Fuente Merino I, Gutierrez Villanueva JL, Celaya González S, et al. Spanish experience on the design of radon surveys based on the use of geogenic information. J Environ Radioat 2017; 166(2): 390–7. doi: doi.org/10.1016/j.jenvrad.2016.07.007

24. Spanish Nuclear Safety Council (CSN). Map of natural gamma radiation in Spain (MARNA) at a scale of 1: 1,000,000. 2001. Available from: https://www.csn.es/mapa-de-radiacion-gamma-natural-marna-mapa [cited 21 October 2020]

25. IGME, Geological and Mining Institute of Spain, Lithostratigraphic Map of Spain, 1:200.000. Available from: http://mapas.igme.es/Servicios/default.aspx#IGME_Litoestratigrafico200 [cited 21 October 2020].

26. European Commission, Joint Research Centre, Cinelli G, De Cort M, Tollefsen T, (Eds.). European atlas of natural radiation. Luxembourg: Publication Office of the European Union; 2019.

27. FOREGS – EuroGeo Surveys. Geochemical Atlas of Europe. Available from: http://weppi.gtk.fi/publ/foregsatlas/index.php [cited 21 October 2020].

28. Reimann C, Birke M, Demetriades A, Filzmoser P, O'Connor P, (Eds.). Chemistry of Europe's agricultural soils - Part A: Methodology and interpretation of the GEMAS data set & Part B: General background information and further analysis of the GEMAS data set. Geologisches Jahrbuch (Reihe B 102 & 103), Hannover: Schweizerbarth; 2014. 322 pp. & 528 pp. + DVD.

29. Suarez Mahou E, Fernández Amigot JA, Baeza Espasa J, Moro Benito MC, García Pomar D, Moreno Del Pozo J, Lanaja Del Busto J. CSN Technical Reports Collection 5.2000. INT-04-02. Marna Project. Map of natural gamma radiation, Nuclear Safety Council (CSN), Madrid, 2000. Legal deposit: M-668-2001, ISBN: 84-95341-12-3

30. Slapansky P, Bieber G, Motschka K, Ahl A, Winkler E, Schattauer I. Aerophysikalische Vermessung im Bereich Bad Leonfelden (OÖ), Endbericht, ÜLG-20/12a & 13a, ÜLG-28/12a & 13a, Vienna: Geological Survey of Austria (GBA); 2014.

31. IGME Geological and Mining Institute of Spain, One Geology Map of Spain, 1:1M. Available from: http://mapas.igme.es/gis/rest/services/oneGeology/ESP_1M_IGME_1GEGeology_EN/MapServer [cited 21 October 2020].

32. Geological Survey of Austria (GBA), Geological Map of Austria, 1:500.000. Available from: https://www.data.gv.at/katalog/dataset/onegeology-gba [cited 21 October 2020].

33. IGME Geological and Mining Institute of Spain, Karstic Map of Spain, 1:1M. Available from: http://mapas.igme.es/gis/rest/services/Cartografia_Tematica/IGME_Karst_1M/MapServer [cited 21 October 2020].

34. Bundesforschungszentrum für Wald (BFW). Bodenkarte Österreich. Available from: https://bodenkarte.at [cited 21 October 2020].

35. Gruber V, Baumann S, Himmelbauer K, Laubichler C, Alber O, Ciotoli G, et al. Radon mapping exercise. Final report of MetroRADON Activity 4.4.2, 16ENV10-MetroRADON. Linz: AGES; 2020.

36. Wood SN. Generalized additive models: an introduction with R. Second Edition. Chapman & Hall/CRC Texts in Statistical Science. Boca Raton: CRC Press; 2017.

37. Borgoni R, De Francesco D, De Bartolo D, Tzavidis N. Hierachical modelling of indoor radon concentration: how much do geology and building factors matter? J Environ Radioact 2014; 138: 227–37. doi: 10.1016/j.jenvrad.2014.08.022

38. JP Chilès, Delfiner P. Geostatistics: modeling spatial uncertainty. 2nd edition. New York, NY: Wiley; 2012.

39. Wackernagel H. Multivariate Geostatistics: an introduction with applications. 3rd edition. Berlin: Springer-Verlag; 2003.

40. Isaaks E, Srivastava R. An introduction to applied geostatistics. New York, NY: Oxford University Press Inc., 1989; 561 p.

41. Neznal M, Neznal M, Matolín M, Barnet I, Mikšová J. The new method for assessing the radon risk of building sites. Czech Geological Survey Special Papers 16. Prague: Czech Geological Survey; 2004, p. 48. Available from: https://www.radon-vos.cz/pdf/metodika.pdf

42. Krivoruchko K. Empirical Bayesian Kriging. Redlands, CA: Esri. Available from: http://www.esri.com/news/arcuser/1012/empirical-byesian-kriging.html [cited 04 November 2020]

43. Krivoruchko K, Gribov A. Evaluation of empirical Bayesian kriging. Spatial Stat 2019; 32. doi: 10.1016/j.spasta.2019.100368

44. Cinelli G, Tondeur F, Dehandschutter B, Development of an indoor radon risk map of the Walloon region of Belgium, integrating geological information. Environ Earth Sci 2011; 62(4): 809–819. doi: 10.1007/s12665-010-0568-5

45. Tondeur F, Cinelli G. A software for indoor radon risk mapping based on geology. Nucl Tech Radiat Protect 2014; XXIX: S59–63.

46. Cinelli G, Tondeur F. Log-normality of indoor radon data in the Walloon region of Belgium. J Environ Radioact 2015; 143: 100. doi: 10.1016/j.jenvrad.2015.02.014

47. AFCN. Belgium Radon Map. Available from: https://afcn.be/fr/dossiers-dinformation/radon-et-radioactivite-dans-votre-habitation/radon#Taux de radon dans votre commune [cited 21 October 2020].

*Valeria Gruber
Austrian Agency for Health and Food Safety (AGES)
Department for Radon and Radioecology
Wieningerstrasse 8
4020 Linz, Austria
Email: valeria.gruber@ages.at